https://doi.org/10.5194/egusphere-2025-258
Preprint. Discussion started: 24 February 2025

The 21st-century wetting inhibits growing surface ozone in Northwestern China

Authors: Xiaodong Zhang[1,*], Yu Yan[2], Ning Zhang[2], Wenpeng Wang[3], Huabing Suo[2], Xiaohu Jian[1], Chao Wang[2], Haibo Ma[2], Hong Gao[2,*], Zhaoli Yang[2], Tao Huang[2], Jianmin Ma[1]

Affirmations:

[1] Laboratory for Earth Surface Processes, College of Urban and Environmental Sciences, Peking University, Beijing, 100871, P. R. China

[2] Key Laboratory for Environmental Pollution Prediction and Control, Gansu Province, College of Earth and Environmental Sciences, Lanzhou University, Lanzhou, 730000, P.R. China

[3] College of Atmospheric Sciences, Lanzhou University, Lanzhou, 730000, P.R. China

[*] **Corresponding author:** Xiaodong Zhang, email: zhangxd2020@pku.edu.cn; Hong Gao, email: honggao@lzu.edu.cn

ABSTRACT:

Previous studies have shown that surface air temperature (SAT) facilitates the formation of surface ozone (O_3), while relative humidity (RH) often inhibits ozone generation. However, the degree to which O_3 may respond simultaneously to rising SATs and RH due to climate change remains less understood. We conducted extensive atmospheric chemistry model scenario simulations to investigate the impacts of long-term trends of humidification and warming on summer O_3 concentrations in Northwestern China (NW) from 1998 to 2017, a period during which this region experienced both warming and the most significant wetting trend in China. We found that the summer mean O_3 level in NW increased by 19.9% during this time. The changes in meteorology led to a reduction in O_3 levels, primarily due to humidification in NW, which counteracts the warming-induced O_3 increase. We demonstrate that the wetting trend in NW will continue from 2019 to 2030 under a shared socioeconomic pathway (SSP) in conjunction with a representative concentration pathway SSP5-RCP8.5, but will either cease or shift to drier conditions from 2019 to 2060 under the SSP2-RCP4.5. No significant responses of O_3 fluctuations to RH variations were observed, partly due to manual intervention under the SSP2-RCP4.5.

Keywords: Ozone, Wetting, Warming, Northwestern China, Future projection

https://doi.org/10.5194/egusphere-2025-258
Preprint. Discussion started: 24 February 2025

1. Introduction

Atmospheric humidity is recognized as a crucial factor that directly and indirectly influences the formation and evolution of surface ozone (Ghazali et al., 2022; Han et al., 2011; Kerr et al., 2020). The relationship between atmospheric humidity and surface O_3 is complex. From a chemical standpoint, humidity can modify the rates of photochemical reactions, thereby affecting O_3 formation. Additionally, humidity plays a role in generating hydroxyl radicals (OH) in the atmosphere, which are vital for breaking down volatile organic compounds (VOCs) and other pollutants (Ding et al., 2023; Ma et al., 2021). These radicals can interact with O_3 precursors, impacting the rate of O_3 production. High humidity can also enhance aerosol formation, facilitating heterogeneous reactions. Depending on the specific chemical pathways involved, some of these reactions may either generate or deplete O_3 (Eck et al., 2020). From a physical perspective, humidity is critical for cloud and fog formation as well as precipitation. The latter promotes O_3 dissolution in water droplets and its removal from the atmosphere through wet deposition, particularly during precipitation events, which weakens solar radiation and disrupts the energy balance near the surface (Ding et al., 2021; Eck et al., 2020; Kleeman, 2008; Madden and Williams, 1978; Millstein and Harley, 2009).

It has been reported that O_3 levels increased by 30% over Northern China in summer and 50% over Eastern China in autumn during a dry year compared to a wet year, indicating that wet climate conditions do not support rising O_3 levels (Ding et al., 2023). Long-term ambient O_3 measurement data indicate that rising absolute air humidity resulted in lower near-surface O_3 concentrations at temperatures of 0−30°C (Belan and Savkin, 2019). Other studies examining the relationship between O_3 concentrations and atmospheric humidity have also identified negative correlations between O_3 levels and humidity (Li et al., 2022). Nevertheless, significant knowledge gaps regarding the relationship between humidity and O_3 persist (Li et al., 2021). Most previous studies utilized short-term or instantaneous O_3 concentrations to evaluate the associations between O_3 and atmospheric humidity (Gong et al., 2021; Li et al., 2021). Their long-term relationships still require clarification. Previous investigations of the connections between climate and O_3 primarily focused on the impact of air temperature, which often overshadows the effects of other meteorological variables (Wang et al., 2024). The extent to which atmospheric humidity could significantly influence the long-term O_3 trend remains uncertain, given that the synergistic effects of warming and wetting frequently occur in a warming climate. In this context, O_3 and RH trends in NW over

https://doi.org/10.5194/egusphere-2025-258
Preprint. Discussion started: 24 February 2025

the past decades likely present a unique scenario to help bridge this knowledge gap. NW (Fig. S1), located in the hinterland of the Asian-European continent, is Asia's largest arid and semi-arid region, characterized by limited rainfall and vegetation (Koster et al., 2004; Yang et al., 2023). Meteorological records indicate that from 1960 to 2013, precipitation in NW increased at a rate of 0.55 mm per year (Li et al., 2012; Liu et al., 2013; Yang et al., 2017). During this period, the air temperature rose at a rate of 0.034 °C per year, exceeding the warming trends observed across all of China (0.025 °C per year) and globally (0.013 °C per year). Although RH does not exhibit a significant growth trend during this period, in the recent decade (2008-2017), it increased markedly at a slope of 0.313 in NW and 0.381 in the three westernmost provinces of Xinjiang, Gansu, and Qinghai within NW. Based on these records, NW appears to be entering a "warming and wetting" phase, accompanied by a rise in precipitation, runoff, and lake levels (Nie et al., 2022; Peng and Zhou, 2017; Shi et al., 2002; Yao et al., 2021).

The present study aims to address the knowledge gap in the complex and long-term relationships between ozone pollution and atmospheric humidity, focusing on NW, where increasing O_3 pollution, air temperature, and humidity have co-occurred (Peng and Zhou, 2017; Yang et al., 2017), mainly since the early 2000s. This research provides valuable insights into the broader context of air quality management and climate variability by enhancing our understanding of the long-term relationship between ozone pollution and atmospheric humidity.

2. Method and data

2.1 WRF-Chem Model Configuration

Since measured O_3 concentration data in China is only available after 2013, we applied the three-dimensional Weather Research and Forecasting with Chemistry (WRF-Chem) version 3.7 model (http://www2.mmm.ucar.edu/wrf/users/wrf_files/wrfv3.7/updates-3.7.html) to predict meteorology, O_3 concentrations, and other relevant data in Northwestern and mainland China. The model domain spans the entire mainland China at a 20 km × 20 km resolution, extending vertically from the surface to the lower stratospheric ozone layer at an altitude of 50 hPa with 30 staggered vertical layers. This vertical segmentation facilitates a deepened comprehension of the O_3 dynamics within the region, enabling the capture of its detailed behavior throughout the

https://doi.org/10.5194/egusphere-2025-258
Preprint. Discussion started: 24 February 2025

atmospheric stratifications (Li et al., 2020; Zhang et al., 2020, 2022). Detailed physical and chemical schemes contributing to O_3 formation in WRF-Chem and emission input followed previous studies (Bei et al., 2018; Bossioli et al., 2016; Liao et al., 2015; Tie et al., 2009; Wild et al., 2000) and are presented in Section S1 in the Supplement and Tables S1-S2. The soil NO, NO_x, and HONO emissions have been considered a necessary process contributing to surface ozone formation in recent years (Lu et al., 2021). However, given the lack of soil emission inventories of these reactive nitrogen species in China and the world, the present modeling study did not take these processes into consideration. The aerosol feedback mechanisms include the direct and indirect effects, the both are considered in WRF-Chem. The model simulations with a nudging option in WRF were conducted from June 1st to August 31st in each summer from 1998 to 2017, with a time-step of 30s. A spin-up time of three days was adopted before June 1st in each summer. Further details are referred to Section S1 in the Supplement.

2.2 Trend

Considering relatively short data time series (1998-2017), the Mann-Kendall (MK) Test and Sen's slope (El-Shaarawi and Niculescu, 1992; Kendall, 1949; Mann, 1945) were used to examine the trend of O_3, near-surface air temperature (SAT) at the 2m height, and relative humidity (RH, %) at the 2m height. The Mann-Kendall (MK) Test and Sen's Slope are both non-parametric statistical methods commonly used for analyzing trends in time series data. The MK Test helps determine if there is a significant trend, and Sen's slope quantifies the strength and direction of the trend (slope value).

2.3 O_3 Attribution to Meteorology and Emission

We calculated the fraction (percentage change, %) to account for O_3 attribution to meteorology and emission subject to different model scenarios. For example, we define the fraction

$$F_{O3} = (C_{S3} - C_{S1}) / C_{S1} \times 100\%, \quad (1)$$

as the attribution of O_3 concentration to emissions, where C_{S1} and C_{S3} are the summer surface O_3 air concentrations from the base (S1) and fixed meteorology (S3) scenarios.

2.4 Data

https://doi.org/10.5194/egusphere-2025-258
Preprint. Discussion started: 24 February 2025

To initialize and prescribe boundary conditions in the WRF model from 1998 to 2017, meteorological data were sourced from the ERA-Interim reanalysis from the European Centre for Medium-Range Weather Forecast (ECMWF, https://www.ecmwf.int/en/forecasts/datasets/reanalysisdatasets/era-interim).

Anthropogenic emissions were collected from the Emissions Database for Global Atmospheric Research (EDGAR) version 4.3 on a spatial resolution of 0.1° × 0.1°, which was available when we started this modeling investigation. A grid-mapping program implemented the emissions into the WRF-Chem (Crippa et al., 2018; Mo et al., 2017). Biogenic emissions were simulated using MEGAN version 2.1 (Guenther et al., 2006, 2012). A recent study suggests that temperature can alter precursor emissions (Pfannerstill et al., 2024). However, since available emission inventories worldwide, including the widely-used EDGAR inventory, did not account for the influence of meteorology, typically the air temperature, on emissions but only considers emissions from anthropogenic and natural sources, the emissions input in the present modeling might be subject to additional uncertainties. The reduction of these uncertainties will depend on improved inventories that take the meteorological effect into account.

We have replaced WRF land-use change (LUC) data with Chinese land use/land cover remote sensing monitoring database provided by the Data Center for Resources and Environmental Sciences, Chinese Academy of Sciences (RESDC) (http://www.resdc.cn), which significantly improved China's LUC in our investigation of the effect of urbanization on O_3 pollution in China (Zhang et al., 2022). The new LUC data has a spatial resolution of 1 km × 1 km, which is extrapolated to the WRF-Chem grid cells (20 km × 20 km).

Considering that the warming and wetting trends in NW might persist in the coming decades, we also projected future O_3 and meteorology in 2019, 2030, and 2060 in the WRF-Chem model framework and simulations, respectively. We collected future anthropogenic emission data from the Dynamic Projection Model for Emissions in China (DPEC Inventory – MEICModel, http://meicmodel.org.cn), with a spatial resolution of 0.25° × 0.25° longitude and latitude (Cheng et al., 2021, 2023; Tong et al., 2020). The meteorological data was collected from Shared Socioeconomic Pathways (SSP) and Representative Concentration Pathways (RCP) climate scenarios under the CMIP6 framework (https://aims2.llnl.gov/search/cmip6/), with the MPI-ESM1-2-HR model (Eyring et al., 2016). Compared with other models, MPI-ESM1-2-HR has higher resolution and can simulate the complex interactions within the climate system, including

https://doi.org/10.5194/egusphere-2025-258
Preprint. Discussion started: 24 February 2025

all climate scenarios (SSP2-RCP4.5 and SSP5-RCP8.5) targeted by this study, and has been widely used in WRF simulations.

2.5 Model Evaluations

Rigorous comparisons between simulated O_3 concentrations and measured data were conducted and presented in Figs. S2-S7 and Section S2 in the Supplement. Overall, the simulated O_3 concentrations agree reasonably well with measured data, demonstrating a high level of reliability of modeling results.

2.6 Model Scenario Setup

We established several model scenarios to distill signals of meteorological conditions, primarily SAT and RH, in modeled O_3 concentrations. Detailed configurations are provided in Table 1. The first scenario (S1) serves as the baseline, incorporating summer-specific meteorological variables and emissions from 1998 to 2017 into WRF-Chem simulations, and is thus considered a realistic scenario. In the second scenario (S2), we fixed emissions from 1998 throughout the period from 1998 to 2017, aiming to assess the significance of the meteorological effect on O_3 variation. In the third scenario (S3), we fixed meteorology from 1998 during the same period, thereby emphasizing the importance of emissions in O_3 variation. To evaluate the sensitivity of scenario S3, we also conducted an additional WRF-Chem run by fixing SAT and RH only in 1998 (scenario S4) and compared the modeled O_3 concentrations with those simulated in scenario S3 for 2004. The results indicate minor differences between model scenario S3 and the results from the fixed SAT and RH model run (Fig. S8). By calculating the differences and fractions, we can discern the contributions of meteorology and emissions to O_3 formation and destruction. We also established two additional model scenarios to project the responses of O_3 concentrations to future meteorology and emissions in NW based on CMIP6 pathways SSP2-RCP4.5 and SSP5-RCP8.5, specifically for 2019, 2030, and 2060, respectively. Detailed descriptions of these two pathways and the corresponding data are presented in Section S3 in the Supplement.

https://doi.org/10.5194/egusphere-2025-258
Preprint. Discussion started: 24 February 2025

Table 1. Model scenarios.

Scenario	Simulation period	Meteorology	Emission	LUC
S1	1998-2017	Varied	Varied	Varied
S2	1998-2017	Varied	Fixed (1998)	Varied
S3	1998-2017	Fixed (1998)	Varied	Varied
S4	2004	Only fixed SAT and RH (1998)	Varied	Varied
S5	1998-2017	Varied	Varied	Fixed (1998)
SSP2-4.5	2019, 2030, 2060	Varied	Varied	Varied
SSP5-8.5	2019, 2030, 2060	Varied	Varied	Varied

3. Results and Discussion

3.1 Summer Ozone Trends

Figures 1a and 1b present MK-Test statistics and Sen's slope estimated temporal trends of summer O_3 concentrations from 1998 to 2017 under scenario S1 (base scenario) and S3 with fixed meteorology in China. In the S1 scenario (Fig. 1a), O_3 concentrations exhibit statistically significant declining trends in the northernmost regions, spanning from Northeastern Xinjiang to Northeastern China, with the most significant decline occurring in Inner Mongolia. Increasing O_3 concentrations are observed along Tianshan Mountain in Xinjiang, western Tibet, and central China. The fixed meteorology scenario (S3, Fig. 1b) shows a monotonically increasing trend across China, indicating continuously rising O_3 levels for the past two decades due to growing precursor emissions, except for some grid cells in the Yangtze River Delta (YRD), the Pearl River Delta (PRD), the Beijing-Tianjin metropolitan area, and other sporadic regions, where MK-Test and Sen's slope identified statistically significant negative O_3 trends. Previous studies have also noted the negative trends over the past decade in these regions (Hu et al., 2024; Li et al., 2022; Wang et al., 2020; Yu et al., 2021). The Beijing-Tianjin area, YRD, and PRD are three critical regions under China's joint efforts to prevent and control air pollution. Regional emission

https://doi.org/10.5194/egusphere-2025-258
Preprint. Discussion started: 24 February 2025

mitigation in these areas may lead to varying reductions in precursor emissions and declines in O_3 concentrations. Overall, increasing precursor emissions have dominated the O_3 trend in China, as meteorology remained constant during this period. This is evidenced by the linear trends of NOx and NMVOC (Non-methane VOC) emissions in China from 1998 to 2017 (Fig. S9). When comparing the MK-Test and Sen's slope results between the two scenarios model runs, the meteorological conditions from 1998 to 2017 overshadowed the effects of emissions, primarily contributing to the declining O_3 levels (negative trends) in the northernmost regions of China, extending from Inner Mongolia to Northeastern China. Our modeling result shows that mean summer O_3 concentration averaged over Inner Mongolia reached the maximum in 2007 and slightly declined thereafter (Fig. S10). This can be partly attributed to relatively lower precursor emissions resulting from the sparse population and limited industrial activities in this part of China, though having a growing trend (Zhang et al., 2022, 2023).

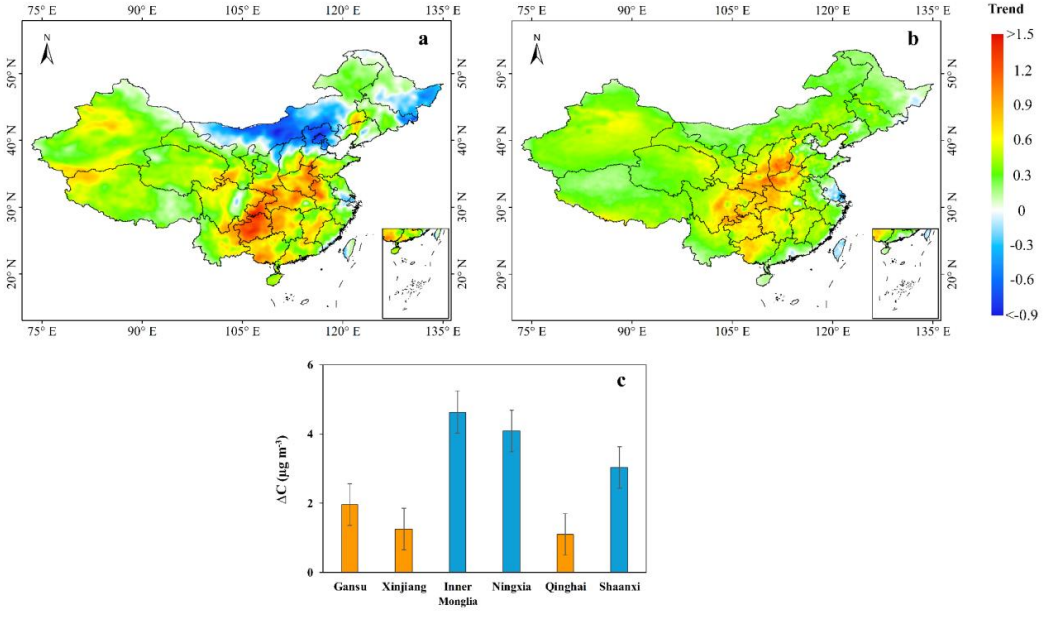

Figure 1. MK-Test and Sen's slope estimated summer O_3 concentration trend and O_3 attribution (fraction or percentage change, %) under baseline (S1) and fixed meteorology (S3) scenarios from 1998 to 2017, respectively. (a) MK-Test and Sen's slope estimated trend from the base scenario S1, the trends of concentrations are well within the MK-Test statistically significant range at 95% confidence level in terms of |Z|>1.96 criteria; (b) same as Fig. 1a but for fixed meteorology scenario S3; (c) mean differences of summer mean O_3 concentrations

https://doi.org/10.5194/egusphere-2025-258
Preprint. Discussion started: 24 February 2025

averaged from 1998 to 2017 between the model scenarios 1 and 3, defined by $\overline{\Delta O_3} = \bar{O}_{3,S1} - \bar{O}_{3,S3}$, where $\bar{O}_{3,S1}$ and $\bar{O}_{3,S3}$ stand for mean summer O_3 concentrations averaged over 1998 to 2017, respectively. $\overline{\Delta O_3}$ in three Westernmost provinces of NW is shown by yellow bars and blue bars for three Easternmost provinces of NW. Error bar in Fig. 1c stands for ±1 STD.

To discern potential influences of meteorology on O_3 concentrations at the provincial level, we estimated the differences of summer mean O_3 concentrations averaged from 1998 to 2017 between model scenarios 1 (S1) and 3 (S3), defined by $\overline{\Delta O_3} = \bar{O}_{3,S1} - \bar{O}_{3,S3}$. Figure 1c illustrates $\overline{\Delta O_3}$ in each province of Northwestern China. Since the mean O_3 levels under scenario S1 were greater than those under scenario S3 with fixed meteorology in 1998, although in some years we also identified negative ΔO_3 in the three westernmost provinces (Xinjiang, Gansu, and Qinghai), we would expect positive $\overline{\Delta O_3}$, as shown in Fig. 1c. In this context, the values of $\overline{\Delta O_3}$ indicate the extent of meteorological influence on O_3 concentrations. Specifically, the smaller $\overline{\Delta O_3}$, the stronger meteorological influences, as a smaller $\overline{\Delta O_3}$ suggests that O_3 levels with varying meteorology (S1) are closer to those with fixed meteorology in 1998 (S3). We highlighted the three provinces with smaller $\overline{\Delta O_3}$ (<2 μg m^{-3}) using yellow bars, all located in Westernmost NW, indicating a weaker increase in O_3 concentrations in these three westernmost provinces compared to others, aligning well with the RH trends in these provinces, as compared to the other three provinces located in the east of NW (Inner Mongolia, Ningxia, and Shaanxi), as mentioned in the Introduction. As shown in Fig. S11, modeled concentration fractions under the S2 model scenario with fixed emissions in 1998 in the three westernmost provinces of NW are negative, indicating that meteorology tended to inhibit the increase in summer ozone concentrations, particularly in Xinjiang, Gansu, and Qinghai, confirming the result in Fig. 1c. In the other three provinces to the east of NW, we observe larger $\overline{\Delta O_3}$ values, suggesting that meteorology, along with precursor emissions, tended to enhance O_3 levels from 1998 to 2017. Consequently, we would expect that meteorology favored O_3 growth in these three eastern provinces of NW.

3.2 Associations of summer ozone with wetting and warming

https://doi.org/10.5194/egusphere-2025-258
Preprint. Discussion started: 24 February 2025

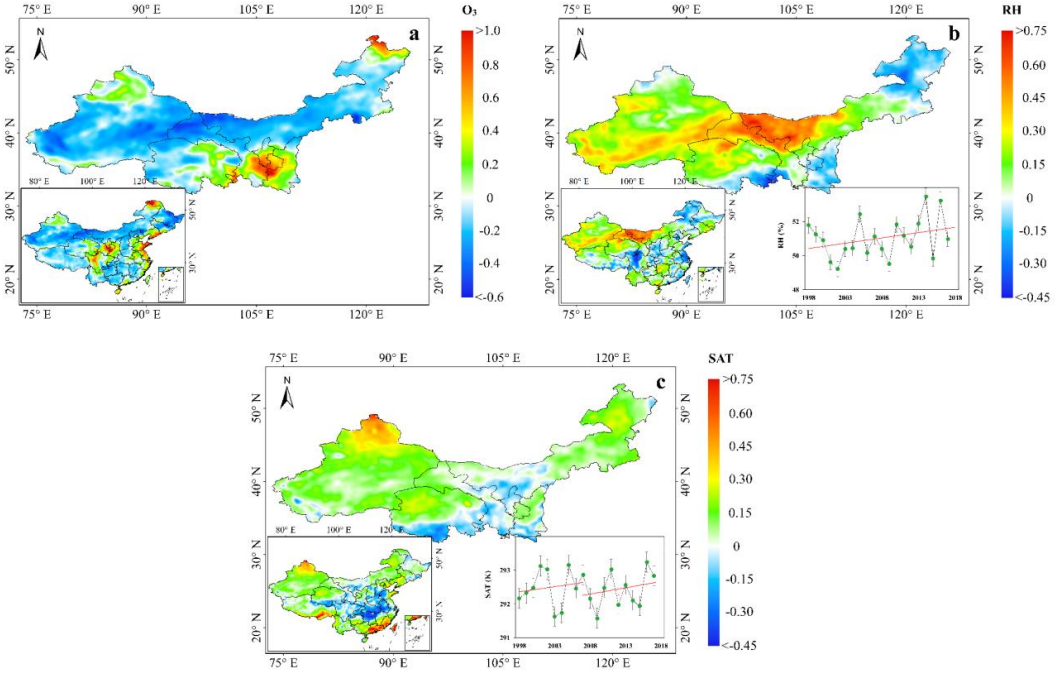

Figure 2. (a) MK-Test statistics for the trends of summer O_3 concentrations from 1998 to 2017 subject to model scenario 2 (S2) with fixed emissions in 1998, (b) MK-Test statistics for summer RH from 1998 to 2017, the line chart on the low-right corner illustrates summer RH in NW from 1998 to 2017 under scenario 2, (c) MK-Test statistics for trend of summer SATs from 1998 to 2017, the line chart shows summer SATs averaged over Northwest China from 1998 to 2017, under scenario 2. Contour figures on the low left corner of Figs. 2a-2c illustrates MK-Test statistics for O_3 trends under fixed emission (model scenario 2) and modeled RH and SAT trends in mainland China from 1998 to 2017. The trends are well within the statistically significant range at 95% confidence level in terms of |Z|>1.96 criteria.

Figure 2a illustrates the MK-Test statistics of gridded summer O_3 concentrations from 1998 to 2017 subject to the model scenario S2 with fixed emissions and annually varied meteorology, aiming to highlight the effect of meteorology on O_3 evolution. A notable decline in summer O_3 ozone concentrations is evident in most areas of mainland China, except for the Northern China Plain, central China, the Sichuan Basin, and the Guanzhong Plain (inner figure on the left-low corner of Fig. 2a). The declining O_3 trends are also evident in most regions across NW with the most substantial decrease occurring in west Gansu, northwest Inner Mongolia, and Xinjiang. With fixed emission, such an O_3 falling trend is induced primarily by meteorology (climate). Considering that air temperature and humidity are two key meteorological factors influencing O_3 fluctuations, we present the MK-Test statistics of the trends of summer relative humidity (RH, %)

https://doi.org/10.5194/egusphere-2025-258
Preprint. Discussion started: 24 February 2025

at the 2 m height in Northwestern and mainland China (illustrated in the lower-left corner of Fig. 2b), along with their annual variations depicted in a line chart in the lower-right corner of Fig. 2b. We also present the surface air temperature (SAT, K) in Northwestern and mainland China in a line chart in the lower-right corner of Fig. 2c. Compared to many places across Eastern and Central China where RH has negative or drying trends (left-low corner of Fig. 2b), RH in NW showed a marked surge, suggesting pronounced wetting, as reported before (Peng and Zhou, 2017). This can also be seen in the annual changes in the mean RH averaged over NW (the line chart on the right-low corner of Fig. 2b) from 1998 to 2017, dominated by an overall upward RH trend with a mean growth rate of 1.9% per year. Likewise, NW also experienced warming during the same period, as shown in Fig. 2c, particularly in the western part of NW, including Xinjiang, western Gansu Province, and Qinghai Province. NW has been undergoing one of the most significant warming trends in the nation. Between 2005 and 2017, NW, particularly the Xinjiang region, has warmed by over 0.5 K with a rate of 0.04 K/yr. In contrast, eastern and Central China show a cooling trend. The rising SAT trend and falling O_3 trend are in contrast to the common knowledge that increasing SATs should enhance O_3 levels. The result thus implies that SATs did not dominate the O_3 trend in NW.

https://doi.org/10.5194/egusphere-2025-258
Preprint. Discussion started: 24 February 2025

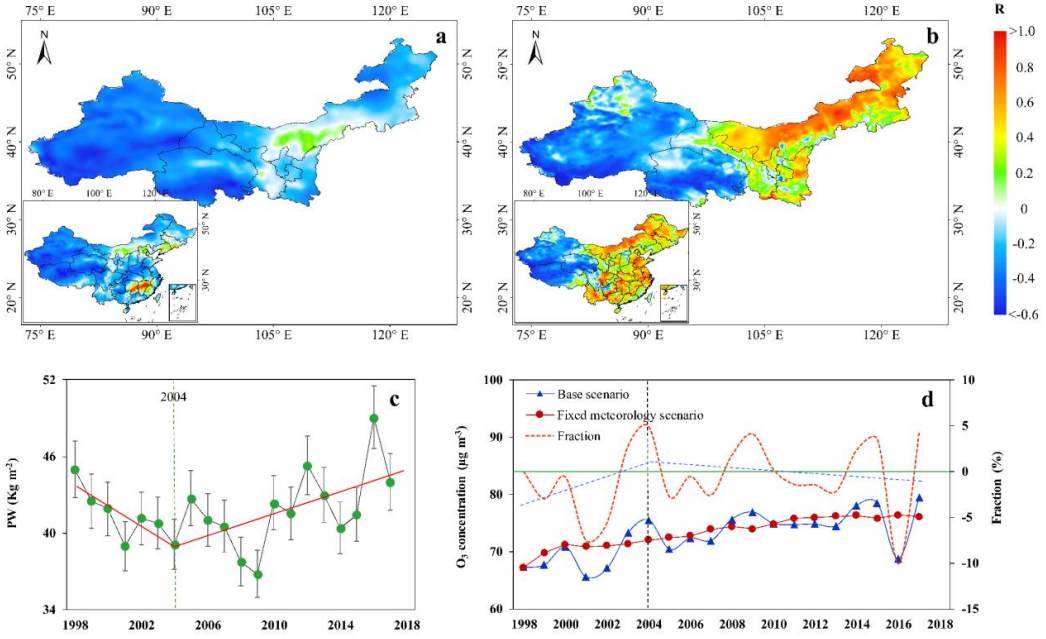

Figure 3. (a) Pearson correlation (R) between summer O_3 concentration and RH from 1998 to 2017 under S2 scenario, (b) R between summer OH radical concentration and O_3 concentration from 1998 to 2017 under S2 scenario, (c) summer surface precipitable water (PW) in the bounded area of NW from 1998 to 2017, error bar stands for ±1 STD and red solid line stands for linear trend, (d) summer O_3 concentrations under Scenarios 1 (dark blue solid line with triangles) and 3 (red solid line with circles) scaled on the left-Y axis, and their fractions $F_{O3} = (C_{S1} - C_{S3}) / C_{S3} \times 100\%$ (red dashed line) in three Westernmost provinces of HW (Xinjiang, Qinghai, and Gansu), where C_{S1} and C_{S3} are the summer (June to August) surface O_3 air concentrations from the base (S1) and fixed meteorology (S3) scenarios, scaled on the right-Y axis, the blue dashed line in Fig. 3d is a linear fitting line from 1998 to 2004 and 2004 to 2017, respectively. The green solid line represents the zero-value line of the fraction.

As mentioned earlier, since rising temperatures favor O_3 formation while increasing humidity is detrimental to O_3 growth, it is intriguing to investigate which of these two meteorological factors contributes more to the O_3 trend in NW. We first calculated linear correlation coefficients between RH and O_3 concentrations modeled from the S2 scenario (fixed emissions) from 1998 to 2017 across Northwestern and mainland China (bottom left corner of Fig. 3a). Strong negative correlations are evident in most regions of Xinjiang, Qinghai, and Western Gansu. These negative correlations indicate declining O_3 concentrations with rising RH. To highlight the influences of RH and precipitation on summer O_3 variation, Fig. 3d illustrates modeled mean summer O_3 concentrations averaged over three Westernmost provinces of HW (Xinjiang, Qinghai, and Gansu)

https://doi.org/10.5194/egusphere-2025-258
Preprint. Discussion started: 24 February 2025

under the base scenario S1 with annually varying summer meteorology and emissions, and S3 with fixed meteorology in 1998 and annually varying emissions averaged over NW, along with the concentration fractions (%, red dashed line) between the two scenarios from 1998 to 2017. O_3 concentrations exhibit the same increasing trend primarily driven by rising precursor emissions. However, the S1 scenario shows more significant annual fluctuations (solid dark blue line in Fig. 3d) compared to the S3 scenario (solid red line in Fig. 3d). These stronger fluctuations can be attributed to the influence of meteorology. Since scenarios 1 and 3 shared the same emissions and chemistry, the concentration fractions quantify the contributions of meteorology to the O_3 trend alone. As shown, the fractions increased from 1998 to 2004, decreased thereafter, and turned negative since 2009 (the red dashed lines), indicating that meteorology has led to declining O_3 concentrations since 2005 in NW. Among the two key meteorological factors influencing O_3 formation, increasing SAT (Fig. 2c) tends to elevate O_3 levels, which contradicts the decreasing and negative O_3 fractions. Consequently, RH likely plays a more significant role in the O_3 trend in NW, as rising RH aligns well with the decreasing and negative O_3 fractions.

Figure 3c displays the mean summer surface precipitable water (PW, kg/m2) over the region bounded between 75 – 100°E in Northwest China from 1998 to 2017, collected from the NCAR reanalysis (https://psl.noaa.gov/cgi-bin/data/composites/printpage.pl). One can identify a slow decrease in PW from 1998 to 2004 and a rapidly growing PW thereafter. Since warming exacerbates drought in arid and sub-arid NW (Lian et al., 2021), growing precipitation in NW implies that increasing humidity might play a more significant role than warming in the changing climate, which acts to reduce O_3 levels via precipitation washout and chemistry. A close look at Figs. 2b, 2c, and Fig. 3a indicate that more substantial warming and wetting occurred in Xinjiang, Gansu (including westernmost of Inner Mongolia), and Qinghai provinces. We compared the fractions of provincial mean summer RH and summer O_3 concentrations from the fixed emissions and annually varying meteorology scenario (S2) between 1998 and 2017 (Fig. 4a), defined by $f = (Y_{2017} - Y_{1998}) / Y_{1998} \times 100\%$, where f is the concentration or RH fractions and Y_{1998} and Y_{2017} stand for O_3 concentrations or RH in 1998 and 2017, respectively, thereby to highlight the net effect from meteorology. The most significant fraction of O_3 concentration was identified in Inner Mongolia at 9.9%, followed by Ningxia (5.7%), Shaanxi (5.5%), Gansu (2.8%), Xinjiang (1.6%), and Qinghai (-1.5%), respectively. Among the six provinces, Xinjiang and Gansu accounted for smaller O_3 fractions, and Qinghai accounted for a negative fraction (Fig. 4a), indicating that O_3

https://doi.org/10.5194/egusphere-2025-258
Preprint. Discussion started: 24 February 2025

levels in these three provinces inclined less significantly or even declined (Qinghai) between 1998 and 2017 than the other three provinces. Interestingly, more significant O_3 fractions, meaning growing O_3 levels for the two decades in Inner Mongolia, Ningxia, and Shaanxi, correspond to smaller (Ningxia) or negative (Inner Mongolia and Shaanxi) RH fractions, meaning falling RH. In contrast, more diminutive and negative O_3 fractions in Xinjiang, Gansu, and Qinghai provinces are associated well with the stronger increasing trend of summer RH by MK-test (Figs. 2b and 4a) at the growing rate of 9.8% in Xinjiang, 8.9% in Gansu, and 9.9% in Qinghai from 1998 to 2017, respectively. While the weak or falling summer O_3 levels in three provinces respond to both growing RH and SAT trends (Fig. 2b and 2c), since growing SATs tend to enhance O_3 concentrations but modeled O_3 respond weakly to rising SAT in these three provinces, the result demonstrates again that the wetting might inhibit O_3 formation and increment for the past decades in NW.

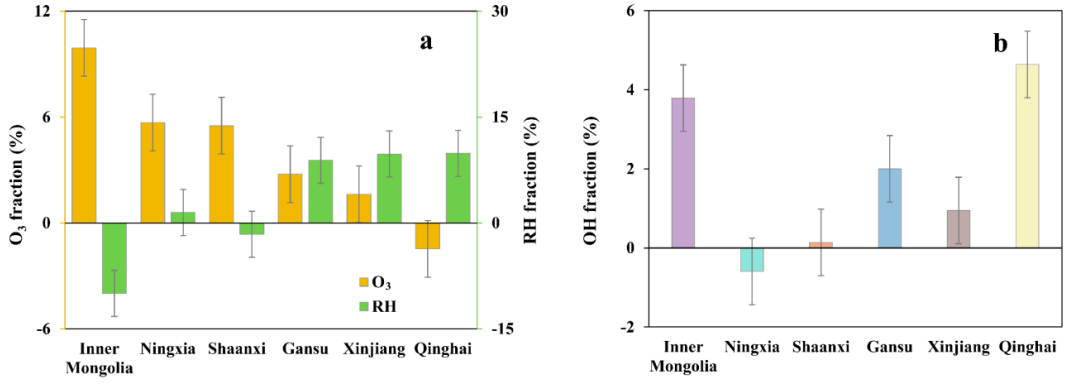

Figure 4. Summer RH, O_3, and OH radical fractions between 1998 and 2017 in six provinces of NW under the fixed emission scenario (S2). (a) RH and O_3 fractions, O_3 fractions are scaled on the left Y-axis, and RH fractions are scaled on the right Y-axis, (b) OH radical fractions. Error bars denote ±1 STD.

It is worthwhile to point out that model scenario 2 with fixed emissions also considers chemistry, in which OH radicals and water vapor can interact. The primary source of OH radicals in the atmosphere is the reaction between water vapor (H_2O) and excited oxygen atoms ($O(^1D)$), which are formed by the photolysis of ozone (O_3) by ultraviolet (UV) radiation. The OH radicals react with ozone to form oxygen (O_2) and the excited oxygen atom $O(^1D)$, which can further react with water vapor to regenerate two OH radicals:

https://doi.org/10.5194/egusphere-2025-258
Preprint. Discussion started: 24 February 2025

$$O_3 + OH \rightarrow O_2 + O(^1D), \quad (2)$$

$$O(^1D) + H_2O \rightarrow 2\ OH.$$

This reaction does not lead to a net reduction in OH radicals but contributes to ozone removal by initiating reactions that lead to the formation of less reactive species. Figure 3b is a correlation diagram between modeled summer O_3 concentrations and OH radicals in NW and mainland China (the left-low corner of Fig. 3b) subject to the fixed emission scenario (S2). The spatial pattern of correlation coefficients in NW is, to some extent, similar to that between O_3 concentrations and RH (Fig. 3a), showing the negative associations between OH radicals and O_3 concentrations, particularly in Xinjiang and Qinghai with the most significant wetting trend, suggesting that increasing OH radicals reduce O_3 levels. Figure 4b displays the fractions of provincial mean summer OH radicals from the fixed emissions and annually varying meteorology scenario (S2) between 1998 and 2017. Relatively larger positive fractions can be discerned in Xinjiang, Qinghai, and Gansu, meaning increasing OH radicals in these provinces as a result of increasing RH (Eq. 1), which corresponds to higher RH fractions and lower O_3 fractions. An exception occurs in Inner Mongolia, where the large positive OH radical fraction (Fig. 4b) is associated with negative RH and large O_3 fractions (Fig. 4a). OH radicals show an increasing trend (Fig. S12) which agrees with the positive correlation between OH and O_3 concentrations shown in Fig. 3b. This puzzling from the modeling results needs further investigations.

There are several primary mechanisms of OH radicals leading to O_3 reduction, including the reaction with VOCs to form peroxyl radicals (RO_2), the reaction of RO_2 with nitrogen oxides (NO_x = NO + NO_2) to form nitrogen dioxide (NO_2) and other compounds, and photodissociation of NO_2. Figures S9a and S9b show the MK test estimated NO_x and NMVOC emission trends from 1998 to 2017. While increasing NO_x is observed in NW (Fig. S9a), its emission levels are considerably lower than in Eastern and Southern China (Fig. S9c). Both NMVOC emission levels and trends in NW are significantly smaller than in Eastern and Southern China due to lower populations and less developed economies (Fig. S9b and S9d). Hence, it is likely that the reaction of water vapor (H_2O) with excited oxygen atoms ($O(^1D)$) produced by the photodissociation of ozone by UV light plays a specific role in the negative correlation between O_3 and OH radicals.

A multiple regression model (MRM) was established to further quantitatively assess the contribution of RH and SAT to summer O_3 concentrations in NW. The MRM has been applied in

https://doi.org/10.5194/egusphere-2025-258
Preprint. Discussion started: 24 February 2025

a number of investigations to quantify meteorological effects on ozone evolution in China (Li et al., 2019, 2020, 2021; Yan et al., 2024). For SAT and RH, the MRM model can be defined as

$$\ln(O_3) = \alpha + \beta_1 \ln(SAT) + \beta_2 \ln(RH) + \varepsilon, \quad (3)$$

where α, β_1, and β_2 are model coefficients, and ε is a random error, respectively. In the first instance, we considered three provinces with significant wetting trends: Xinjiang, Gansu, and Qinghai. We combined annual summer O_3, RH, and SAT from three provinces into one time series of each dependent and independent variable from 1998 to 2017, yielding 60 samples for each variable. Tables S4-S6 present regression coefficients and statistics of the MRM. To examine the multicollinearity in the MRM, we estimated the variance inflation factor (VIF, Table S4-S6). The VIFs for RH and SAT are far less than 10, indicating no multicollinearity in the model. The contribution of RH and SAT to O_3 is calculated by:

$$\text{Contribution}_i = \frac{\left|\beta_i \times \frac{STD_i}{STD_\alpha}\right|}{\text{SUM}}, \quad (4)$$

where $\text{SUM} = \sum_i |\beta_i \times STD_i/STD_\alpha|$, and β_i denotes the regression coefficient of independent variable i (namely, RH and SAT), STD_i is the standard deviation of regression coefficient of independent variable i, and STD_α represents the standard deviation of coefficient of intercept.

The MRM analysis reveals that RH contributes 77.5%, 59.4%, and 46.2% to O_3 variations in Xinjiang, Qinghai, and Gansu. Accordingly, SAT contributes 22.5%, 40.6%, and 53.8% to O_3 fluctuations in these three provinces from 1998 to 2017. The results indicate that RH has become a major contributor to long-term change in O_3 concentrations, overwhelming or equivalent to SAT's contributions to the O_3 trend for the past two decades, likely via interactions among increasing precipitation washout and OH radical, O_3 concentration, and water vapor.

We further assess the contributions of precipitation, RH, SAT, winds, and PBLH (planetary boundary-layer height) to O_3 evolution in NW using an extended MRM model. The results confirm that RH and SAT made the most significant contributions to long-term ozone trends than other meteorological variables under the long-term perspective. As seen from Fig. 5, the contribution of RH (49.5%) and SAT (47.6%) to O_3 evolution in NW was almost equivalent (Fig. 5a), but the SAT (92.4%) dominated in entire mainland China (Fig. 5b). Whereas the PBLH only contributed

https://doi.org/10.5194/egusphere-2025-258
Preprint. Discussion started: 24 February 2025

about 2% to O_3 variations because the PBLH varies on a daily and hourly basis and affects insignificantly (summer) seasonal changes in O_3 concentrations.

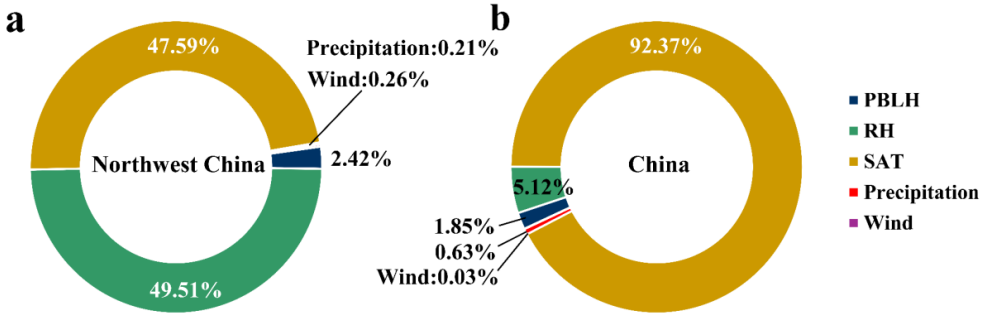

Figure 5. Contribution of PBLH (planetary boundary-layer height), RH, SAT, precipitation, and wind to O_3 evolution. (a) Northwest China, (b). Mainland China.

It should be pointed out that since the wetness also helps growing vegetation, which causes increasing biogenic VOC emission (BVOC) and hence rising O_3 concentrations, the contribution of BVOCs to O_3 fluctuations under increasing wetness should also be taken into consideration. To examine this hypothesis, we designed an extra model scenario (S5) in which we used the updated LUC data (section 2.4) and fixed LUC in 1998 in the WRF-Chem simulation and ran the model from 1998 to 2017. Since the LUC defines vegetation coverage, the fixed LUC suggests no vegetation change during this period. We then estimated the fractions between modeled O_3 concentration with fixed LUC and the baseline scenario S1 with annually-varying LUC, thereby eliminating the effects from emissions, meteorology, and chemistry but highlighting the LUC (or greenness) effect only. The result is illustrated in Fig. S13. As shown, while the fraction fluctuates positively (Xinjiang) and negatively (Northern Shaanxi and Eastern Inner Mongolia), indicating increasing and decreasing O_3 levels induced by LUC or greening, the magnitudes of provincial mean concentration fractions are very small, mostly ranging from -1% to 0.3%, suggesting that the LUC under the wetting trend in NW plays an insignificant role in O_3 fluctuation.

3.3 Projected future climate impacts on summer Ozone

https://doi.org/10.5194/egusphere-2025-258
Preprint. Discussion started: 24 February 2025

Given the significant impacts of wetting on O_3 evolution in NW over the past two decades, concerns have also been raised regarding O_3 responses to future wetting and warming. We estimated the projected O_3 concentrations, RH, and SAT fractions between the baseline and fixed meteorology scenarios under the SSP2-4.5 and SSP5-8.5 pathways (section 2.6) for the years 2019, 2030, and 2060, respectively (Figs. 6 and 7). As mentioned earlier, since both scenarios implemented the same emissions and chemistry but the baseline scenario accounted for variable meteorology, the fractions (or differences) between the two scenarios eliminated the effects of emissions and chemistry, thereby isolating meteorological signals only.

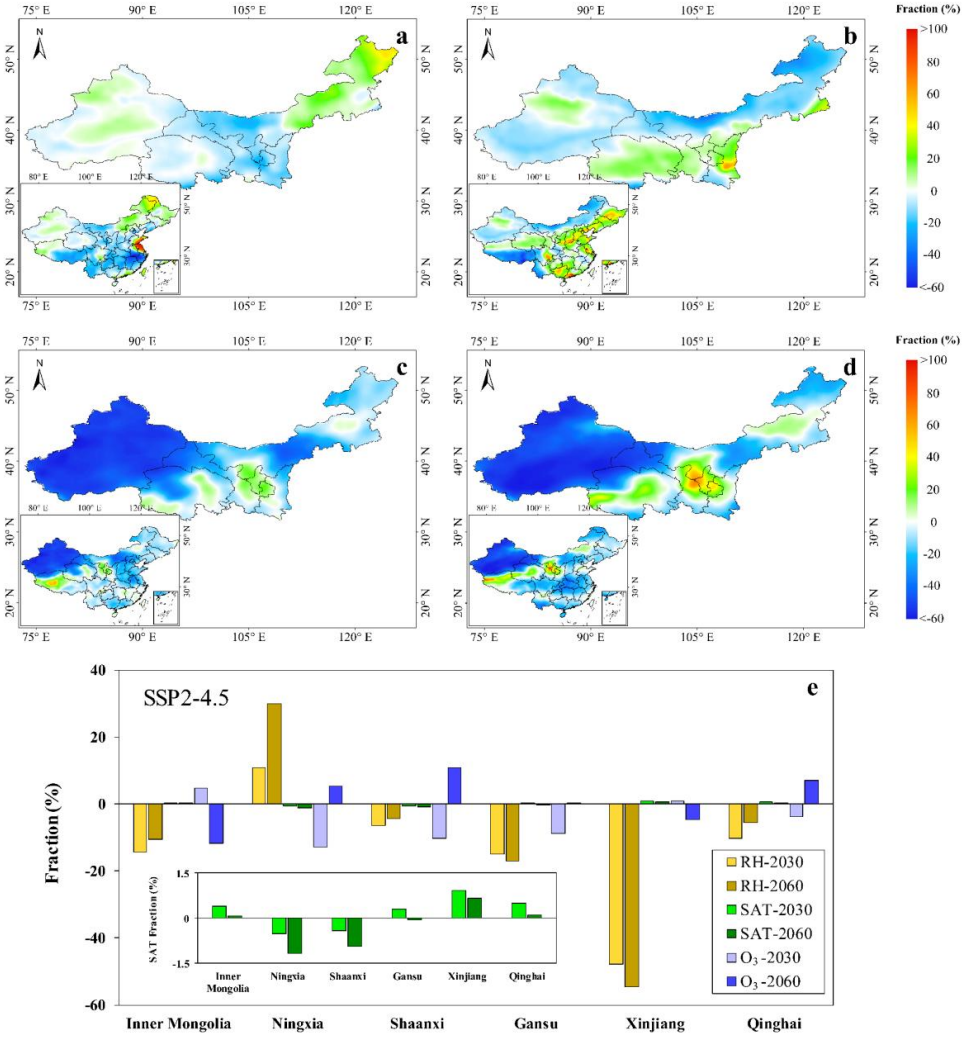

https://doi.org/10.5194/egusphere-2025-258
Preprint. Discussion started: 24 February 2025

Figure 6. (a) Summer O_3 concentration fractions of 2019 to 2030 under SSP2-4.5scenario, estimated by $F_{SSP245} = (C_{2030} - C_{2019}) / C_{2019} \times 100\%$, where C_{2019} and C_{2030} are the summer surface O_3 air concentrations in 2019 and 2030, respectively, (b) same as Fig. 6a but for O_3 fractions of 2019 to 2060, (c) same as Fig. 6a but for summer RH fractions of 2019 to 2030, (d) same as Fig. 6a but for summer RH fractions of 2019 to 2060, (e) fractions of RH, SAT, and O_3 of 2019 to 2030 and 2019 to 2060 (shown in the same color bar as 2030 but with oblique lines) in the six provinces of Northwestern China under the SSP2-4.5 scenario.

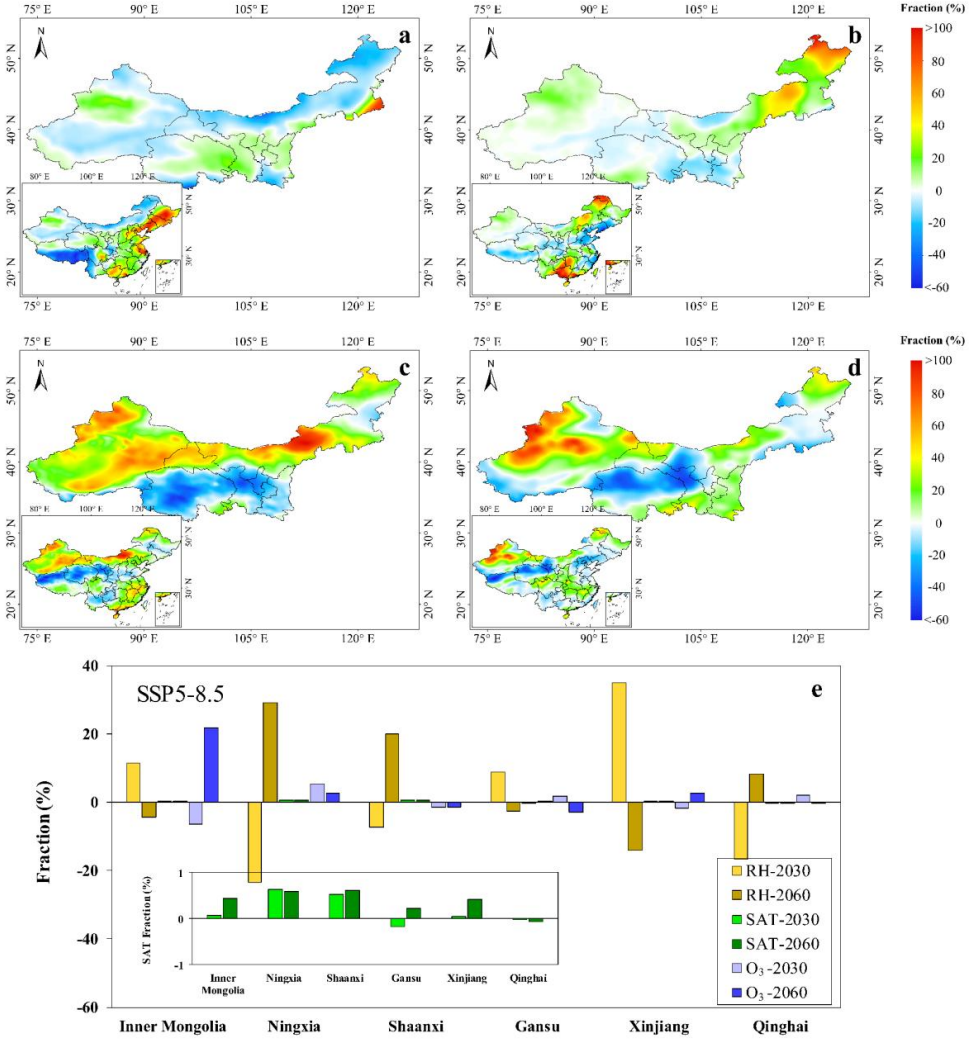

Figure 7. (a) Summer O_3 concentration fraction of 2019 to 2030 under the SSP5-8.5 scenario, estimated by $F_{SSP585} = (C_{2030} - C_{2019}) / C_{2019} \times 100\%$, where C_{2019} and C_{2030} are the summer surface O_3 air concentrations in 2019 and 2030, respectively, (b) same as Fig. 7a but for O_3 fraction of 2019 to 2060, (c) same as Fig. 7a but for summer RH fraction of 2019 to 2030, (d) same as Fig. 7a but for summer RH fraction of 2019 to 2060, (e)

https://doi.org/10.5194/egusphere-2025-258
Preprint. Discussion started: 24 February 2025

fractions of RH, SAT, and O_3 of 2019 to 2030 and 2019 to 2060 (shown in the same color bar as 2030 but with oblique lines) in the six provinces of Northwestern China under the SSP5-8.5 scenario.

Detailed discussions on the associations between projected O_3 evolution and trends of RH and SAT under the SSP2-4.5 and SSP5-8.5 pathways from 2019 to 2030 and from 2019 to 2060 are presented in Section S4 in the Supplement and Figs. 6-7 and Fig. S14, respectively. Overall, from 2019 to 2030, we observe a stronger negative association between O_3 and RH under SSP5-8.5 than under SSP2-4.5 across NW, suggesting that climate conditions under the SSP5-8.5 scenario will more effectively suppress O_3 growth compared to SSP2-4.5 during this period. However, from 2019 to 2060, the SSP5-8.5 tends to project higher O_3 levels than SSP2-4.5. From a wetting trend perspective, we must determine which pathway would project a more realistic future humidity trend in NW. China has been making significant strides in transitioning to renewable energy sources, reducing its carbon footprint, and committing to achieve a carbon peak before 2030 and carbon neutrality by 2060. These commitments align more closely with the mitigation efforts outlined in SSP2-4.5, which, as manual interventions, will overshadow the impact of climate change on O_3 fluctuations. There have also been debates regarding ongoing wetting trends in NW based on CMIP6 projections under SSP5-8.5 and historical data analysis (Huang et al., 2017). Historically, China's rapid economic growth has heavily depended on fossil fuels, which may render SSP5-8.5 more applicable in China. The responses of O_3 evolution to RH under SSP5-8.5 are more akin to those observed from 1998 to 2017 (section 3.2) than to SSP2-4.5. In light of this, while China may achieve its carbon peak and neutrality goals, the wetting trend in NW will likely persist in the coming decades, exacerbating continuous O_3 pollution in NW, in addition to manual interventions.

4. Conclusions

This study conducted extensive sensitivity model simulations to explore the surface O_3 responses to past and future climate change in Northwestern China. The results demonstrated that significant wetting since the 21st century in this region, particularly in the three westernmost provinces (Xinjiang, Qinghai, and Gansu) of NW, has slowed O_3 growth. We show that in these provinces, the wetting influence on O_3 evolution has outweighed the warming effect and played an almost equal role to warming across the entire NW. Both factors contributed approximately 50%

https://doi.org/10.5194/egusphere-2025-258
Preprint. Discussion started: 24 February 2025

to summer O_3 variations from 1998 to 2017, among the major meteorological factors causing changes in O_3 concentrations. This finding contrasts with the dominant role of warming in the meteorological effects on O_3 evolution in China. We linked the increasing OH radicals, which interact with water vapor, to the declining O_3 trend. Given that humidification in NW is projected to continue in the coming years and that the mitigation of O_3 precursor emissions in China will still be implemented under the nation's air pollution control strategies, the impact of humidification on O_3 trends in NW will likely become more significant. Such an impact should be considered in future policymaking for the reduction of O_3 pollution in NW.

Data availability

ERA-Interim reanalysis data can be accessed at https://www.ecmwf.int/en/forecasts/datasets/reanalysisdatasets/era-interim. EDGAR dataset is available at https://edgar.jrc.ec.europa.eu/. LUC data can be accessed at http://www.resdc.cn. DPEC Inventory is available at http://meicmodel.org.cn. The meteorological data under the CMIP6 framework is collected from https://aims2.llnl.gov/search/cmip6/.

Author contributions

XZ and YY contribute equally to this article. All authors contributed to the manuscript and have given approval of the final version. XZ and HG coordinated and supervised the project. XZ, YY, WW and JM designed the present experiment, carried out modeling, and drafted the manuscript. NZ, HS, XJ, CW, and HM collected the data. XZ, YY, ZY and TH analyzed simulation results.

Competing interests

The authors declare that they have no known competing financial interests or personal relationships that could have appeared to influence the work reported in this paper.

Acknowledgements

We wish to thank the High-performance Computing Platform of Peking University to support extensive model simulations of this study.

Financial support

This research was supported by the National Natural Science Foundation of China via grants 42407134, 42177351 and 41977357.

References

https://doi.org/10.5194/egusphere-2025-258
Preprint. Discussion started: 24 February 2025

Bei, N. F., Zhao, L. N., Wu, J. R., Li, X., Feng, T., and Li, G. H.: Impacts of sea-land and mountain-valley circulations on the air pollution in Beijing-Tianjin-Hebei (BTH): A case study, Environ. Pollut., 234, 429–438, https://doi.org/10.1016/j.envpol.2017.11.066, 2018.

Belan, B. D., and Savkin, D. E.: The Role of Air Humidity in Variations in Near-Surface Ozone Concentration, Atmospheric and Oceanic Optics, 32, 586–589, https://doi.org/10.1134/S1024856019050038, 2019.

Bossioli, E., Tombrou, M., Kalogiros, J., Allan, J., Bacak, A., Bezantakos, S., Biskos, G., Coe, H., Jones, B. T., Kouvarakis, G., Mihalopoulos, N., and Percival, C. J.: Atmospheric composition in the Eastern Mediterranean: Influence of biomass burning during summertime using the WRF-Chem model, Atmos Environ., 132, 317–331, https://doi.org/10.1016/j.atmosenv.2016.03.011, 2016.

Cheng, J., Tong, D., Zhang, Q., Liu, Y., Lei, Y., Yan, G., Yan, L., Yu, S., Cui, R. Y., Clarke, L., Geng, G. N., Zheng, B., Zhang, X. Y., Davis, S. J., and He, K. B.: Pathways of China's $PM_{2.5}$ air quality 2015-2060 in the context of carbon neutrality, Natl. Sci. Rev., 8, nwab078, https://doi.org/10.1093/nsr/nwab078, 2021.

Cheng, J., Tong, D., Liu, Y., Geng, G. N., Davis, S. J., He, K. B., and Zhang, Q.: A synergistic approach to air pollution control and carbon neutrality in China can avoid millions of premature deaths annually by 2060, One Earth, 6, 978–989, https://doi.org/10.1016/j.oneear.2023.07.007, 2023.

Crippa, M., Guizzardi, D., Muntean, M., Schaaf, E., Dentener, F., van Aardenne, J. A., Monni, S., Doering, U., Olivier, J. G. J., Pagliari, V., and Janssens-Maenhout, G.: Gridded emissions of air pollutants for the period 1970-2012 within EDGAR v4.3.2, Earth Syst. Sci. Data, 10, 1987–2013, https://doi.org/10.5194/essd-10-1987-2018, 2018.

Ding, J., Dai, Q., Zhang, Y., Xu, J., Huangfu, Y., and Feng, Y.: Air humidity affects secondary aerosol formation in different pathways, Sci. Total Environ., 759, 143540, https://doi.org/10.1016/j.scitotenv.2020.143540, 2021.

Ding, J., Dai, Q., Fan, W., Lu, M., Zhang, Y., Han, S., and Feng, Y.: Impacts of meteorology and precursor emission change on O_3 variation in Tianjin, China from 2015 to 2021, J. Environ. Sci., 126, 506–516, https://doi.org/10.1016/j.jes.2022.03.010, 2023.

Ding, S., Jiang, X., and Wu, C.: Contrasting Near-Surface Ozone Pollution in Wet and Dry Year over China, Int. J. Environ. Res. Public Health, 20, 998, https://doi.org/10.3390/ijerph20020998, 2023.

Eck, T. F., Holben, B. N., Kim, J., Beyersdorf, A. J., Choi, M., Lee, S., Koo, J. H., Giles, D. M., Schafer, J. S., Sinyuk, A., Peterson, D. A., Reid, J. S., Arola, A., Slutsker, I., Smirnov, A., Sorokin, M., Kraft, J., Crawford, J. H., Anderson, B. E., Thornhill, K. L., Diskin, G., Kim, S. W., and Park, S.: Influence of cloud, fog, and high relative humidity during pollution transport events in South Korea: Aerosol properties and $PM_{2.5}$ variability, Atmos. Environ., 232, 117530, https://doi.org/10.1016/j.atmosenv.2020.117530, 2020.

Eyring, V., Bony, S., Meehl, G. A., Senior, C. A., Stevens, B., Stouffer, R. J., and Taylor, K. E.: Overview of the Coupled Model Intercomparison Project Phase 6 (CMIP6) experimental design and organization, Geosci. Model Dev., 9, 1937–1958, https://doi.org/10.5194/gmd-9-1937-2016, 2016.

Ghazali, S., Awang, N. R., Karim, M. F. A., and Muhammad, M.: Fluctuational Analysis of Nighttime Ground-Level Ozone Concentrations due to Variations in Hourly Relative Humidity, Smart Environmental Science, Technology and Management, 1, 118–121, https://doi.org/10.36647/978-93-92106-02-6.21, 2022.

Gong, C., Yue, X., Liao, H., and Ma, Y. M.: A humidity-based exposure index representing ozone damage effects on vegetation, Environ. Res. Lett., 16, 044030, https://doi.org/10.1088/1748-9326/abecbb, 2021.

Guenther, A., Karl, T., Harley, P., Wiedinmyer, C., Palmer, P. I., and Geron, C.: Estimates of global terrestrial isoprene emissions using MEGAN (Model of Emissions of Gases and Aerosols from Nature), Atmos. Chem. Phys., 6, 3181–3210, https://doi.org/10.5194/acp-6-3181-2006, 2006.

Guenther, A. B., Jiang, X., Heald, C. L., Sakulyanontvittaya, T., Duhl, T., Emmons, L. K., and Wang, X.: The Model of Emissions of Gases and Aerosols from Nature version 2.1 (MEGAN2.1): an extended and updated

https://doi.org/10.5194/egusphere-2025-258
Preprint. Discussion started: 24 February 2025

framework for modeling biogenic emissions, Geosci. Model Dev., 5, 1471–1492, https://doi.org/10.5194/gmd-5-1471-2012, 2012.

Han, S., Bian, H., Feng, Y., Liu, A., Li, X., Zeng, F., and Zhang, X.: Analysis of the Relationship between O_3, NO and NO_2 in Tianjin, China, Aerosol Air Qual. Res., 11, 128–139, https://doi.org/10.4209/aaqr.2010.07.0055, 2011.

Huang, J. P., Yu, H. P., Dai, A. G., Wei, Y., and Kang, L. T.: Drylands face potential threat under 2 °C global warming target, Nat. Clim. Chang., 7, 417–422, https://doi.org/10.1038/nclimate3275, 2017.

Hu, F., Xie, P., Xu, J., Lv, Y., Zhang, Z., Zheng, J., and Tian, X.: Long-term trends of ozone in the Yangtze River Delta, China: Spatiotemporal impacts of meteorological factors, local, and non-local emissions, J. Environ. Sci., 7,10–33, https://doi.org/10.1016/j.jes.2024.07.017, 2024.

Kendall, M. G.: Rank Correlation Methods, Mathematics, https://doi.org/10.2307/1402637, 1949.

Kerr, G. H., Waugh, D. W., Steenrod, S. D., Strode, S. A., and Strahan, S. E.: Surface Ozone-Meteorology Relationships: Spatial Variations and the Role of the Jet Stream, J. Geophys. Res-Atmos., 125, e2020JD032735, https://doi.org/10.1029/2020JD032735, 2020.

El-Shaarawi, A. H., and Niculescu, S. P.: On kendall's tau as a test of trend in time series data, Environmetrics, 3, 385–411, https://doi.org/10.1002/env.3170030403, 1992.

Koster, R. D., Dirmeyer, P. A., Guo, Z. C., Bonan, G., Chan, E., Cox, P., Gordon, C. T., Kanae, S., Kowalczyk, E., Lawrence, D., Liu, P., Lu, C. H., Malyshev, S., McAvaney, B., Mitchell, K., Mocko, D., Oki, T., Oleson, K., Pitman, A., Sud, Y. C., Taylor, C. M., Verseghy, D., Vasic, R., Xue, Y. K., Yamada, T., and Team, G.: Regions of strong coupling between soil moisture and precipitation, Science, 305, 1138–1140, https://doi.org/10.1126/science.1100217, 2004.

Kleeman, M. J.: A preliminary assessment of the sensitivity of air quality in California to global change, Climatic Change, 87, 273–292, https://doi.org/10.1007/s10584-007-9351-3, 2008.

Li, B., Chen, Y., and Shi, X.: Why does the temperature rise faster in the arid region of northwest China? J. Geophys. Res-Atmos., 117, D16115, https://doi.org/10.1029/2012JD017953, 2012.

Li, J. X., Wang, Z. X., Chen, L. L., Lian, L. L., Li, Y., Zhao, L. Y., Zhou, S., Mao, X. X., Huang, T., Gao, H., and Ma, J. M.: WRF-Chem simulations of ozone pollution and control strategy in petrochemical industrialized and heavily polluted Lanzhou City, NW, Sci. Total Environ., 737, 139835, https://doi.org/10.1016/j.scitotenv.2020.139835, 2020.

Li, K., Jacob, D. J., Liao, H., Shen, L., Zhang, Q., and Bates, K. H.: Anthropogenic drivers of 2013-2017 trends in summer surface ozone in China, Proc. Natl. Acad. Sci. U.S.A., 116, 422–427, https://doi.org/10.1073/pnas.1812168116, 2019.

Li, K., Jacob, D. J., Liao, H., Qiu, Y. L., Shen, L., Zhai, S. X., Bates, K. H., Sulprizio, M. P., Song, S. J., Lu, X., Zhang, Q., Zheng, B., Zhang, Y. L., Zhang, J. Q., Lee, H. C., and Kuk, S. K.: Ozone pollution in the North China Plain spreading into the late-winter haze season, Proc. Natl. Acad. Sci. U.S.A., 118, e2015797118, https://doi.org/10.1073/pnas.2015797118, 2021.

Li, K., Jacob, D. J., Shen, L., Lu, X., De Smedt, I., and Liao, H.: Increases in surface ozone pollution in China from 2013 to 2019: anthropogenic and meteorological influences, Atmos. Chem. Phys., 20, 11423–11433, https://doi.org/10.5194/acp-20-11423-2020, 2020.

Li, L., Liu, N., Shen, L., Zhao, Z., Wang, H., Wang, Y., Li, X., and Ma, Y.: Ozone concentration at various heights near the surface layer in Shenyang, Northeast China, Front. Environ. Sci., 10, 1011508, https://doi.org/10.3389/fenvs.2022.1011508, 2022.

Li, M., Yu, S., Chen, X., Li, Z., Zhang, Y., Wang, L., Liu, W., Li, P., Lichtfouse, E., Rosenfeld, D., and Seinfeld, J. H.: Large scale control of surface ozone by relative humidity observed during warm seasons in China, Environ. Chem. Lett., 19, 3981–3989, https://doi.org/10.1007/s10311-021-01265-0, 2021.

https://doi.org/10.5194/egusphere-2025-258
Preprint. Discussion started: 24 February 2025

Li, X. B., Yuan, B., Parrish, D. D., Chen, D. H., Song, Y. X., Yang, S. X., Liu, Z. J., and Shao, M.: Long-term trend of ozone in southern China reveals future mitigation strategy for air pollution, Atmos. Environ., 269, 118869, https://doi.org/10.1016/j.atmosenv.2021.118869, 2022.

Lian, X., Piao, S. L., Chen, A. P., Huntingford, C., Fu, B. J., Li, L., Huang, J. P., Sheffield, J., Berg, A. M., Keenan, T. F., McVicar, T. R., Wada, Y., Wang, X. H., Wang, T., Yang, Y. T., and Roderick, M. L.: Multifaceted characteristics of dryland aridity changes in a warming world, Nat. Rev. Earth Env., 2, 232–250, https://doi.org/10.1038/s43017-021-00144-0, 2021.

Liao, J. B., Wang, T. J., Jiang, Z. Q., Zhuang, B. L., Xie, M., Yin, C. Q., Wang, X. M., Zhu, J. L., Fu, Y., and Zhang, Y.: WRF/Chem modeling of the impacts of urban expansion on regional climate and air pollutants in Yangtze River Delta, China, Atmos. Environ., 106, 204–214, https://doi.org/10.1016/j.atmosenv.2015.01.059, 2015.

Liu, X., Zhang, D., Luo, Y., and Liu, C.: Spatial and temporal changes in aridity index in northwest China: 1960 to 2010, Theor. Appl. Climatol., 112, 307–316, https://doi.org/10.1007/s00704-012-0734-7, 2013.

Lu, X., Ye, X. P., Zhou, M., Zhao, Y. H., Weng, H. J., Kong, H., Li, K., Gao, M., Zheng, B., Lin, J. T., Zhou, F., Zhang, Q., Wu, D. M., Zhang, L., and Zhang, Y. H.: The underappreciated role of agricultural soil nitrogen oxide emissions in ozone pollution regulation in North China, Nat. Commun., 12, 5021, https://doi.org/10.1038/s41467-021-25147-9, 2021.

Ma, S., Shao, M., Zhang, Y., Dai, Q., and Xie, M.: Sensitivity of $PM_{2.5}$ and O_3 pollution episodes to meteorological factors over the North China Plain, Sci. Total. Environ., 792, 148474, https://doi.org/10.1016/j.scitotenv.2021.148474, 2021.

Madden, R. A., and Williams, J.: The Correlation between Temperature and Precipitation in the United States and Europe, Mon. Weather Rev., 106, 142–147, https://doi.org/10.1175/1520-0493(1978)106<0142:TCBTAP>2.0.CO;2, 1978.

Mann, H. B.: Nonparametric Tests Against Trend, Econometrica, 13, 245, https://doi.org/10.2307/1907187, 1945.

Millstein, D. E., and Harley, R. A.: Impact of climate change on photochemical air pollution in Southern California, Atmos. Chem. Phys., 9, 3745–3754, https://doi.org/10.5194/acp-9-3745-2009, 2009.

Mo, J. Y., Huang, T., Zhang, X. D., Zhao, Y., Liu, X., Li, J. X., Gao, H., and Ma, J. M.: Spatiotemporal distribution of nitrogen dioxide within and around a large-scale wind farm - a numerical case study, Atmos. Chem. Phys., 17, 14239–14252, https://doi.org/10.5194/acp-17-14239-2017, 2017.

Nie, J. S., Wang, W. H., Heermance, R., Gao, P., Xing, L., Zhang, X. J., Zhang, R., Garzione, C., and Xiao, W. J.: Late Miocene Tarim desert wetting linked with eccentricity minimum and East Asian monsoon weakening, Nat. Commun., 13, 3977, https://doi.org/10.1038/s41467-022-31577-w, 2022.

Peng, D., and Zhou, T.: Why was the arid and semiarid northwest China getting wetter in the recent decades? J. Geophys. Res-Atmos., 122, 9060–9075, https://doi.org/10.1002/2016JD026424, 2017.

Pfannerstill, E. Y., Arata, C., Zhu, Q., Schulze, B. C., Ward, R., Woods, R., Harkins, C., Schwantes, R. H., Seinfeld, J. H., Bucholtz, A., Cohen, R. C., and Goldstein, A. H.: Temperature-dependent emissions dominate aerosol and ozone formation in Los Angeles, Science, 384, 1324–1329, https://doi.org/10.1126/science.adg8204, 2024.

Shi, P. Y., Tilgner, M., and Lo, M. K.: Construction and characterization of subgenomic replicons of New York strain of West Nile virus, Virology, 296, 219–233, https://doi.org/10.1006/viro.2002.1453, 2002.

Tie, X., Madronich, S., Li, G., Ying, Z., Weinheimer, A., Apel, E., and Campos, T.: Simulation of Mexico City plumes during the MIRAGE-Mex field campaign using the WRF-Chem model, Atmos Chem. Phys., 9, 4621–4638, https://doi.org/10.5194/acp-9-4621-2009, 2009.

Tong, D., Cheng, J., Liu, Y., Yu, S., Yan, L., Hong, C. P., Qin, Y., Zhao, H. Y., Zheng, Y. X., Geng, G. N., Li, M., Liu, F., Zhang, Y. X., Zheng, B., Clarke, L., and Zhang, Q.: Dynamic projection of anthropogenic

https://doi.org/10.5194/egusphere-2025-258
Preprint. Discussion started: 24 February 2025

emissions in China: methodology and 2015-2050 emission pathways under a range of socio-economic, climate policy, and pollution control scenarios, Atmos. Chem. Phys., 20 (9), 5729–5757, https://doi.org/10.5194/acp-20-5729-2020, 2020.

Wang, J., Li, J., Li, X., Wang, D., and Fang, C.: Relationship between ozone and air temperature in future conditions: A case study in Sichuan basin, China, Environ. Pollut., 343, 123276, https://doi.org/10.1016/j.envpol.2023.123276, 2024.

Wang, Z. B., Li, J. X., and Liang, L. W.: Spatio-temporal evolution of ozone pollution and its influencing factors in the Beijing-Tianjin-Hebei Urban Agglomeration, Environ. Pollut., 256, 113419, https://doi.org/10.1016/j.envpol.2019.113419, 2020.

Wild, O., Zhu, X., and Prather, M. J.: Fast-J: Accurate Simulation of In- and Below-Cloud Photolysis in Surface Chemical Models, J. Atmos. Chem., 37, 245–282, https://doi.org/10.1023/A:1006415919030, 2000.

Yan, D., Jin, Z. P., Zhou, Y. T., Li, M. M., Zhang, Z. H., Wang, T. J., Zhuang, B. L., Li, S., and Xie, M.: Anthropogenically and meteorologically modulated summertime ozone trends and their health implications since China's clean air actions, Environ. Pollut., 343, 123234, https://doi.org/10.1016/j.envpol.2023.123234, 2024.

Yang, P., Xia, J., Zhang, Y. Y., and Hong, S.: Temporal and spatial variations of precipitation in Northwest China during 1960-2013, Atmos. Res., 183, 283–295, https://doi.org/10.1016/j.atmosres.2016.09.014, 2017.

Yang, X. Y., Li, D. W., Yang, Z., Wu, K., Ji, L. Y., Zhou, Z. Q., and Lu, Y. Q.: Revealing historical observations and future projections of precipitation over Northwest China based on dynamic downscaled CMIP6 simulations, Front. Earth Sci., 10, 1090221, https://doi.org/10.3389/feart.2022.1090221, 2023.

Yao, J. Q., Mao, W. Y., Chen, J., and Dilinuer, T.: Recent signal and impact of wet-to-dry climatic shift in Xinjiang, China, J. Geog. Sci., 31, 1283–1298, https://doi.org/10.1007/s11442-021-1898-9, 2021.

Yu, R. X., Liu, M. X., Li, L., Song, J. Y., Sun, R. D., Zhang, G. J., Xu, L., and Mu R. L.: Spatial and Temporal Variation of Atmospheric Ozone Column Concentration and Influencing Factors in the Yangtze River Delta Region in Recent 15 Years, Acta Scientiae Circumstantiae, 41, 770–784, https://doi.org/10.13671/j.hjkxxb.2020.0346, 2021.

Zhang, X. D., Du, J., Zhang, L. M., Huang, T., Gao, H., Mao, X. X., and Ma, J. M.: Impact of afforestation on surface ozone in the North China Plain during the three-decade period, Agric. For. Meteorol., 287, https://doi.org/10.1016/j.agrformet.2020.107979, 107979, 2020.

Zhang, X. D., Jian, X. H., Zhao, Y., Liu, X. R., Chen, K. J., Wang, L. F., Tao, S., Liu, J. F., Huang, T., Gao, H., Liu, Y. J., Zhugu, R. R., and Ma, J. M.: Tropospheric Ozone Perturbations Induced by Urban Land Expansion in China from 1980 to 2017, Environ. Sci. Technol., 56, 6978–6987, https://doi.org/10.1021/acs.est.1c06664, 2022.

Zhang, X. D., Zhugu, R. Y., Jian, X., Liu, X., Chen, K., Tao, S., Liu, J., Gao, H., Huang, T., and Ma, J. M.: Associations of interannual variation in summer surface ozone with the Western Pacific Subtropical High in China from 1999 to 2017, Atmos. Chem. Phys., 23, 15629–15642, https://doi.org/10.5194/acp-23-15629-2023, 2023.